Journal of
Alzheimer's Disease & Parkinsonism

Research Article **OMICS International**

Endothelial Degeneration of Parkinson's Disease is Related to Alpha-Synuclein Aggregation

Panzao Yang[1-3], Xiao-Li Min[1-5], Mojdeh Mohammadi[1-3,6], Clinton Turner[2,7], Richard Faull[2,8], Henry Waldvogel[2,8], Mike Dragunow[1,2] and Jian Guan[1,2*]

[1]Department of Pharmacology and Clinical Pharmacology, Faculty of Medical and Health Sciences, University of Auckland, New Zealand
[2]Centre for Brain Research, Faculty of Medical and Health Sciences, University of Auckland, New Zealand
[3]Liggins Institute, Faculty of Medical and Health Sciences, University of Auckland, New Zealand
[4]Faculty of Clinical Medicine, Yunnan University of Traditional Chinese Medicine, China
[5]The First Affiliated Hospital of Yunnan University of Traditional Chinese Medicine, China
[6]Department of Toxicology and Pharmacology, School of Pharmacy, Hamadan University of Medical Sciences, Hamadan, Iran
[7]Department of Anatomical Pathology, LabPlus, Auckland City Hospital Auckland, New Zealand
[8]Department of Anatomy and Medical Imaging, Faculty of Medical and Health Sciences, University of Auckland, New Zealand

Abstract

Objective: We previously reported that the ability of vascular remodelling is impaired in human Parkinson's disease, leading to endothelial degeneration and vascular dysfunction. Aggregation of α-synuclein is a hallmark of neurodegeneration in Parkinson's disease and inflammation and autophagy may contribute to secondary neuronal degeneration. The current study examined the association between these characteristic pathologies and endothelial cell degeneration in Parkinson's disease.

Methods: The study used the post-mortem grey matter from middle frontal gyrus (MFG) of human Parkinson's disease and age-matched control cases. Immunohistochemical staining of phosphorylated α-synuclein, p62 for autophagy, Human Leukocyte Antigen-antigen D Related (HLA-DR) for activated microglia, Factor VIII for endothelial cells and Neuronal Nuclei for neurons were performed using either tissue microarray or free-floating sections. The expression of these factors were quantified by analysing the images of the stained sections and compared between the Parkinson's disease and the age-matched control groups.

Results: Compared to the control cases the expression of phosphorylated α-synuclein and p62 was increased in Parkinson's disease, whereas both neurons and endothelial cells were significantly reduced, with no changes in the number of microglial cells. The density of phosphorylated α-synuclein was negatively correlated with the total length of endothelial cell associated blood vessels when compared across normal and Parkinson's disease cases combined. However, using double label immunohistochemistry we found that the degree of endothelial cell degeneration in Parkinson's disease was not directly related to the degree of neuronal degeneration and accumulation of phosphorylated α-synuclein.

Conclusion: α-synuclein and autophagy are associated with endothelial degeneration in Parkinson's disease. The degree of endothelial degeneration was not related to the extent of neuronal degeneration, both of which were co-pathological changes in PD brains. Alpha-synuclein-associated endothelial degeneration was also age-related pathology.

Introduction

Parkinson's disease (PD) is a progressive neurodegenerative disorder characterised by motor dysfunction [1]. Cognitive decline and dementia may appear in some cases as the disease progresses [2]. Using post-mortem human brain tissue from PD cases with no evidence of Alzheimer's disease (AD) pathology, our recent research has reported vascular degeneration in PD, where endothelial degeneration has been suggested to be the cause of the loss of capillary networks and functions [3]. The endothelial degeneration in PD has been described in the substantia nigra (SN), caudate nucleus (CN) and the grey matter of middle frontal gyrus (MFG) which show clear neuronal degeneration [3,4]. The normal physiological turnover of endothelial cells involves the balanced loss and regeneration of endothelium. Our recent study has demonstrated impairment of vascular remodelling by showing reduction of pericytes, vascular cell proliferation and the loss of growth factors, for example VEGF, PDGF and increases in IGFBP-2 in the grey matter MFG of human PD brains [5]. The unbalanced endothelial turnover may be the result of an impaired remodelling process or accelerated loss of endothelium.

The retained basement membrane (BM) in PD leads to increased formation of string vessels which may cause secondary neuronal degeneration due to hypoperfusion, but prevent the leakage of the Blood-Brain Barrier (BBB) in a majority of brain lesions [4]. The changes in the BM, thus the BBB leakage may vary in brain regions, for example while there is no BBB leakage in the SN and MFG we found an increase in fibrinogen in the CN with increase of astrocytosis [4].

Neurodegeneration in PD involves increased α-synuclein aggregation [6], inflammation [7], altered autophagy [8,9] and

*Corresponding author: Jian Guan, Department of Pharmacology and Clinical Pharmacology, Faculty of Medical and Health Sciences, University of Auckland, Private Bag 92019, Auckland 1023, New Zealand, Tel: 0064-9-9236134; E-mail: j.guan@auckland.ac.nz

possibly vascular dysfunction, for example the high string vessels related hypoperfusion. Lewy bodies (LBs), the hallmark of PD are mainly composed of aggregates of misfolded α-synuclein, most of which is phosphorylated at the Serine 129 site [10]. Autophagy is responsible for removal of cytoplasmic proteins and organelles where the polyubiquitin-binding protein p62 plays a key role in directing autophagy targets to the autophagosome for destruction [11]. Because p62 itself is also a substrate of autophagy, impairment of autophagy leads to p62 accumulation [12,13]. LBs were recently reported to be associated with p62 that accumulates in cell culture, implying that the α-synuclein aggregates resist degradation and impair autophagy [8]. The roles for inflammation in AD, a small vessel disease have been largely reported [14,15], whereas the involvement of inflammation in neuronal degeneration of PD is controversial [4,7]. The activation of microglia is a commonly used marker for the inflammatory response in the brain [16].

In addition, vascular degeneration and dysfunction is pathogenic and leads to neuronal degeneration in AD [17,18]. Although the potential hypoperfusion may contribute to secondary neuronal degeneration in PD [4], this study investigated whether the endothelial degeneration [3] is the cause or the result of neuronal degeneration by assessing the co-pathology of neuronal and vascular degeneration in the areas with a different extent of neuronal degeneration and PD pathology within the grey matter of the MFG, where there is no PD-related BBB leakage [4]. Due to limited supply of post-mortem tissues from brain regions with degeneration, we only evaluated the grey matter of MFG in this study which has clear neuronal [4] and endothelial degeneration [3]. More importantly the region is larger than other regions with degeneration and the degree of degeneration throughout the region of interest can be largely variable which allows us to compare the degree of endothelial degeneration with extent of neuronal degenerations. The current study evaluated changes of phosphorylated α-synuclein (pα-synuclein), autophagy, microglia and their activation, and their relationship to endothelial degeneration in human PD cases. The relationships of vessel changes to α-synuclein aggregation and neuronal survival were also compared based on the degrees of neuronal degeneration and α-synuclein pathology.

Methods

This study has received approval from the University of Auckland Human Participants Ethics Committee (Reference number 2008/279).

Tissue preparation and case selections

The tissue preparation procedures for both the tissue microarray (TMA) [5,19] and free-floating sections [3,4,19] have been described previously. Briefly, the brains were provided by the Neurological Foundation of New Zealand Douglas Human Brain Bank. The Formalin fixed tissue came from brains that were perfused first with 1% sodium nitrite and then with 15% formalin in 0.1 M phosphate buffer solution. Brain regions were dissected into blocks. The blocks used for pathological examination and TMA production were embedded in paraffin. The blocks used for making free-floating tissue sections were post-fixed and cryoprotected by transferring the blocks sequentially into 20% and 30% sucrose solution before they were stored at -80°C. The TMA block was sectioned at a thickness of 7 μm. The free-floating blocks were sectioned at 50 μm and stored at 4°C.

The criteria for case selection have also been previously described [4,5]. Briefly, only pathologically diagnosed idiopathic PD cases without dementia and age-matched control cases without significant

pathological changes were selected. All the brains from the selected cases have a PM delay below 48 h. Lists including age, sex, PM delay and cause of death are provided (Tables 1 and 2). Information such as duration and clinical diagnosis are listed for PD cases (Table 1). This study used paraffin embedded tissue microarray (TMA) sections

Case	Age	Sex	PM Delay (h)	Disease Duration (year)	Clinical Diagnosis	Cause of Death
PD10	70	M	NA	NA	Idiopathic PD	Pulmonary embolism
PD11	69	F	36	NA	Idiopathic PD	Perforated gastric ulcer
PD12	76	F	3	NA	Idiopathic PD	*E. coli* septicaemia
PD13	70	M	12	NA	Idiopathic PD	Pneumonia
PD14	81	M	11	NA	Idiopathic PD	Pneumonia,
PD16	79	M	8.5	NA	Idiopathic PD	Pneumonia
PD20	73	M	14	NA	Idiopathic PD	Congestive heart failure
PD21	79	F	9.5	NA	Idiopathic PD	PD
PD23	78	F	18.5	NA	Idiopathic PD	Pneumonia
PD27	77	M	4	NA	Idiopathic PD	End stage PD
PD28	76	F	27	NA	Idiopathic PD	Pneumonia
PD30	82	M	19	11	Idiopathic PD	Multi-organ failure
PD31	67	M	25	NA	Idiopathic PD	Respiratory failure
PD33	91	M	4	7	Idiopathic PD	Pneumonia
PD34	75	F	10	11	Idiopathic PD	Cerebrovascular accident
PD35	73	M	16	16	Idiopathic PD	Pneumonia
PD36	78	F	22	NA	Idiopathic PD	Pneumonia
PD37	81	M	4	13	Idiopathic PD	PD
PD42	83	M	21	14	Idiopathic PD	Myocardial infarction
PD46	77	M	34	18	Idiopathic PD	Pneumonia
PD48	84	M	20	13	Idiopathic PD	NA

NA: Not Available

Table 1: Clinical information of the PD cases.

Case	Age	Sex	PM Delay (h)	Cause of Death
H127	59	F	21	Pulmonary embolus
H137	77	F	12	Coronary atherosclerosis
H139	73	M	5.5	IHD
H144	76	M	18.5	Ruptured aortic aneurysm
H150	78	M	11	Ruptured myocardial infarction
H152	79	M	18	Congestive heart failure
H153	76	M	8	IHD
H154	71	M	23	IHD
H156	89	M	19	Atherosclerosis
H169	81	M	24	CO poisoning
H180	73	M	33	IHD
H181	78	F	20	Aortic aneurysm
H190	72	F	19	Ruptured myocardial infarction
H191	77	M	20	IHD
H193	71	M	23	IHD
H196	85	M	15	Metastatic adenocarcinoma - colon
H198	67	F	27	IHD
H202	83	M	14	Ruptured abdominal aortic aneurysm
H204	66	M	9	IHD
H215	67	F	23.5	IHD

NA: Not Available; IHD: Ischemic Heart Disease

Table 2: Clinical information of the age-matched controls.

containing grey matter of the MFG from 17 PD and 17 age-matched control cases and free-floating tissue sections of the MFG from 9 PD and 6 age-matched control cases.

Immunohistochemistry

TMA sections: TMA sections were used for both peroxidase-DAB immunohistochemistry and double-labelled fluorescent immunohistochemistry. DAB-peroxidase immunohistochemistry was performed using antibodies directed against alpha synuclein (phospho S129) (1:500; Abcam, Melbourne, Australia) [20] and p62 (1:100; BD Biosciences, CA, USA) for macrophagy [21]. The double-labelled fluorescent immunohistochemistry was performed using antibodies directed against Iba1 (1:100; Abcam, Melbourne, Australia) for microglia [22] and Human Leukocyte Antigen - antigen D Related (HLA-DR, 1:200, Dako Corporation, Carpinteria, CA, USA) for activated microglia [23]. The experimental procedures have been described previously [3,19]. All washes, unless noted specifically, were carried out three times for five minutes each in phosphate buffer solution (PBS). All antibodies were diluted with 1% donkey serum (v/v) in PBST (0.2% Triton X-100 (v/v) in PBS).

The TMA sections were incubated at 60°C for one hour and de-paraffinized in two changes of xylene, ten minutes each. The sections were then rehydrated through a graded alcohol series and three changes of water. Antigen retrieval was performed by heating the sections in 10 mM Tris-EDTA buffer with pH9 using a 2100 Retriever (Prestige Medical). For DAB-peroxidase immunohistochemistry, endogenous peroxidase was deactivated by incubating the sections in a solution containing 50% methanol (v/v) and 1% hydrogen peroxide (v/v) for twenty minutes. The sections were then washed and incubated in the primary antibodies for 48 h at 4°C followed by washes and incubation with biotinylated secondary donkey anti-mouse or donkey anti-rabbit antibodies (1:500; Jackson ImmunoResearch Laboratories, West Grove, PA, USA) for twenty four hours at 4°C. The sections were washed and incubated with ExtrAvidin-HRP (1:1000; Sigma-Aldrich Corporation, Saint Louis, MO, USA) for 3 h at room temperature followed by washes and incubation in 0.05% DAB (w/v) solution for 10-20 min to generate a brown reaction product. After that, the sections were dehydrated through a graded alcohol series and three changes of xylene before cover-slipping. For fluorescent immumohistochemistry, the section was incubated in a mixture of goat anti-Iba1 and mouse anti-HLA-DR primary antibodies for 48 h at 4°C. The section was washed and incubated with secondary donkey anti-goat IgG Alexa 594 and donkey anti-mouse IgG Alexa 488 antibodies (1:400; Invitrogen Corporation, Carlsbad, CA, USA) for 24 h at 4°C. The section was then washed before auto-fluorescence reduction by incubating in 0.1% Sudan Black B (w/v) in 70% ethanol (v/v) for 5 min. The section was briefly washed twice in PBST, 20 s each before it was cover-slipped with Prolong Gold antifade reagent (Molecular Probes, Eugene, OR, USA) and sealed with nail polish. The slide was stored at 4°C in the dark before imaging.

Free-floating sections: Free-floating sections of the MFG were used for double colour peroxidase-DAB immunohistochemical staining of endothelial cells with neurons and pα-synuclein, respectively. Antibodies against Factor VIII (1:1000, Dako Corporation, Carpinteria, CA, USA) [3], Neuronal Nuclei (NeuN) (1:1000, EMD Millipore Corporation, Billerica, MA, USA) [4] and α-synuclein (phospho S129) (1:3000, Abcam Melbourne, Australia) [20] were used to label endothelial cells, neurons and pα-synuclein, respectively. Endothelial cells were stained brown, and neurons and pα-synuclein were stained black. The methods were based on previous publications [3,4,19]. All

washes were carried out three times for ten minutes each in PBST. All antibodies were diluted with 1% donkey serum (v/v) in PBST.

Firstly, endogenous peroxidase was deactivated by incubating the sections in a 50% methanol (v/v) solution containing 1% hydrogen peroxide (v/v) for 20 min. The sections were then washed and incubated in the primary antibodies against NeuN or pα-synuclein for 48 h at 4°C followed by washes and incubation with biotinylated donkey anti-rabbit (1:2000, Sigma-Aldrich Corporation, Saint Louis, MO, USA) or donkey anti-mouse (1:1000, Sigma-Aldrich Corporation, Saint Louis, MO, USA) antibodies for twenty four hours at 4°C. The sections were then incubated with ExtrAvidin-HRP (1:1000, Sigma-Aldrich Corporation, Saint Louis, MO, USA) for four hours at room temperature. Black NeuN and pα-synuclein staining was visualized by incubating the sections in DAB-nickel solution containing 0.05% Ammonium Nickel sulphate (w/v). After the DAB-nickel reaction, the experiment was repeated from the endogenous peroxidase deactivation step, following by incubation in the Factor VIII antibody, secondary antibody and ExtrAvidin-HRP as described above. The staining of factor VIII was visualized with DAB solution to generate brown stain. Finally, the sections were mounted, air-dried, dehydrated through a graded alcohol series and xylene and cover-slipped.

Image processing and analysis

Fluorescently labelled TMA sections: For the fluorescently stained TMA sections, the automated VSlide scanner (MetaSystems) was used to obtain 16-bit grayscale images for each colour (Alexa 594 and Alexa 488) with a 20x objective lens. Ten random sampled images were selected from each core for image analysis. A macro was developed in MetaMorph™ software (Molecular Devices) based on the method described in previous publications to analyse the images [24,25]. Briefly, the images were directly processed by the "Neurite Outgrowth" algorithm which segmented the cell bodies and processes of the microglia. The "Neurite Outgrowth Summary Log" was configured to count the number of microglia.

Peroxidase-DAB stained sections: Methods for image analysis have been described previously [4,5]. Briefly, the peroxidase-DAB images were captured using the Nikon E800 microscope equipped with a digital camera (MBF Bioscience) as described previously [4]. Briefly, images of DAB single or double labelling were obtained from each section by automatic randomized sampling. For TMA single labelled sections, ten randomly images were selected from each section for image analysis. For double labelled sections, nine images (3 images x 3 sections) per case were selected randomly for image analysis.

The number and average size of the pα-synuclein and p62 profiles from the TMA images were analysed using macros developed in ImageJ software (V1.50) which enables automatic high throughput image processing. The images were first converted into 8-bit format and background was subtracted. The "Threshold" tool was used to select the targets of interest and create binary images. The number and average size of both pα-synuclein and p62 profiles were obtained using the "Analyse Particles" tool.

For analysing DAB double labelled images the changes of Factor VIII positive endothelium with either NeuN positive neurons or pα-synuclein positive profiles were analysed in the same microscopic images. The number of NeuN positive neurons and pα-synuclein were analysed using macros developed in ImageJ (V1.50). The "Colour Space Converter" plugin in ImageJ was used to convert the original RGB images to grayscale HSB images to segment the black objects. These images were converted into 8-bit format and thresholded to

select the targets of interest and create binary images. The numbers of both neurons and pα-synuclein were obtained by using the "Analyse Particles" tool.

To measure the total length of Factor VIII positive blood vessels, the "line" tool in ImageJ was used to manually trace and measure the blood vessels. The total length of the blood vessels was calculated by adding up the length of all the tracing lines in that image. The average length of vessels was calculated by dividing the total length of the vessels by the number of vessels in that image.

Statistical analysis: The difference between the age-matched control and PD cases was analysed by using two-tailed unpaired t-test. Two-way ANOVA was used to analyse the difference between the age-matched control and PD cases at locations with different densities of pα-synuclein and neurons, where Bonferroni multiple comparison test was performed to compare the differences between the groups and between severities of degeneration. Correlation between vascular density and pα-synuclein density was analysed by using Pearson correlation test, where the r value represents the Pearson correlation coefficient. P values less than 0.05 were considered as statistically significant.

Results

Neuronal and endothelial degeneration, phosphorylated α-synuclein and p62

Unpaired t-tests showed that the density (number/mm^2) of neurons ($p < 0.01$, Figure 1A) and the total length of endothelial cell associated blood vessels ($p < 0.0001$, Figure 1C) were significantly reduced in the PD cases compared to the age-matched controls while the density (number/mm^2) of pα-synuclein profiles were significantly increased in PD ($p < 0.001$, Figure 1B). Furthermore, a Pearson correlation test

showed that the total length of endothelial cell associated blood vessels is negatively correlated with the density of pα-synuclein profiles in the brain ($r = -0.6384$, $p < 0.05$, Figure 1D). When the measurements only included LBs larger than 7 μm^2, unpaired t-test showed that the density ($p < 0.0001$, Figure 2A) and average size ($p < 0.01$, Figure 2B) of the LBs were significantly increased in PD compared to the age-matched controls. Similar increase in the density ($p < 0.0001$, Figure 2C) and average size ($p < 0.0001$, Figure 2D) of the pα-synuclein profiles smaller than 7 μm^2 were also observed in PD.

Immunofluorescent labelling of pα-synuclein was observed in large round shaped inclusions and fibrous structures resembling cellular processes in the PD brain (Figures 3B and 3E). The big round shaped pα-synuclein positive inclusions were located inside neuron-like cells and were morphologically identified as LBs (Figure 3B) and the fibrous structures were identified as Lewy neurites (Figures 3B and 3E). The fluorescent labelling of p62 was observed in inclusions with different sizes known as p62 bodies (Figures 3A and 3D). The study also showed LB-like p62 aggregates, a few of which showed co-localisation with pα-synuclein (Figure 3C) and the others did not (Figure 3F).

Although no difference in the density (Figure 4A) of p62 staining was found between the two groups, the average size of p62 bodies was larger in the PD cases compared to the control cases ($p < 0.05$, Figure 4B). When only the p62 bodies larger than 7 μm^2 were included, there was no difference in the density (Figure 4C) of the large p62 bodies between the two groups, but the average size of the large p62 bodies was increased in the PD cases ($p < 0.05$, Figure 4D). When only the p62 bodies smaller than 7 μm^2 were included, no difference was found in the density (Figure 4E) or average size (Figure 4F) of the small p62 bodies between the two groups.
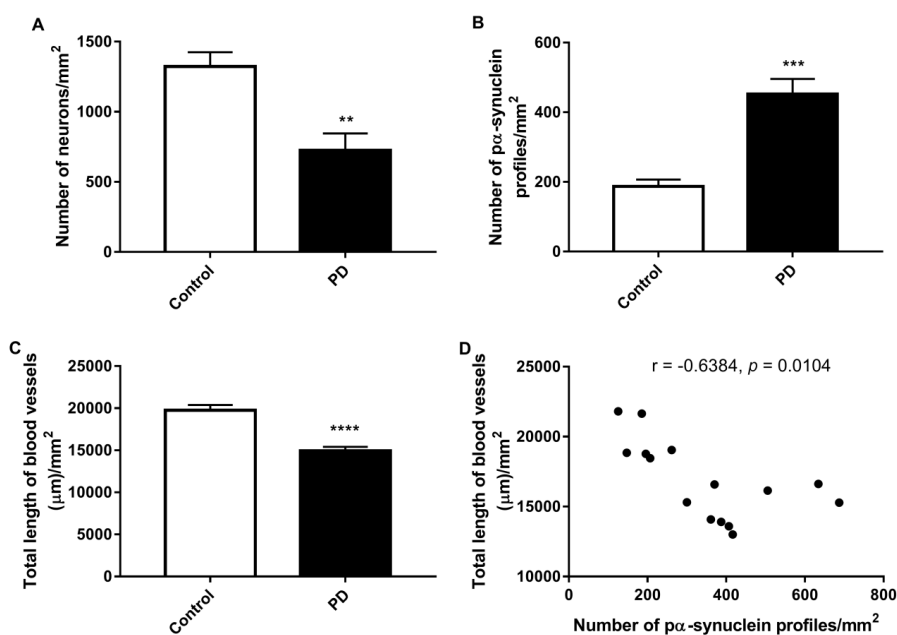

Figure 1: (A) Densities (number/mm^2) of neurons and (B) pα-synuclein profiles and (C) total length of endothelial cell associated blood vessels in the PD and age-matched control cases, and (D) the correlation between the total blood vessel length and the pα-synuclein density. Compared to the age-matched controls, density of neurons (A, **$p<0.01$) and total length of endothelial cell associated blood vessels (C, ****$p<0.0001$) were significantly reduced in the PD cases and density of pα-synuclein profiles was significantly increased in PD (B, ***$p<0.001$). The total length of endothelial cell associated blood vessels was negatively correlated with the density of pα-synuclein profiles in the PD and control brains (D, r=-0.6384, *$p<0.05$).
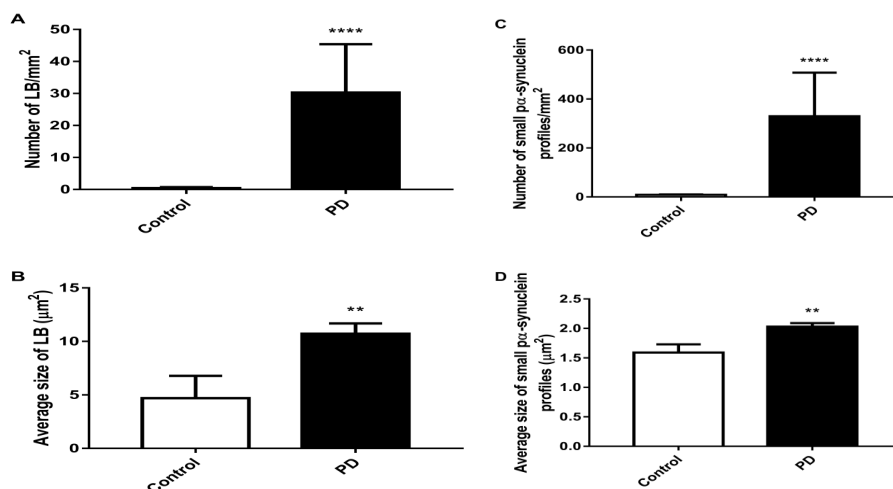
Figure 2: Densities (number/mm^2) and average sizes of the LBs larger than 7 µm^2 and pα-synuclein profiles smaller than 7 µm^2 in the PD and age-matched control cases. Compared to the age-matched control cases, the densities (A, ****$p<0.0001$; C, ****$p<0.0001$) and average sizes (B, **$p<0.01$; D, **$p<0.01$) of both the LBs larger than 7 µm^2 and pα-synuclein profiles smaller than 7 µm^2 were increased in the PD cases.
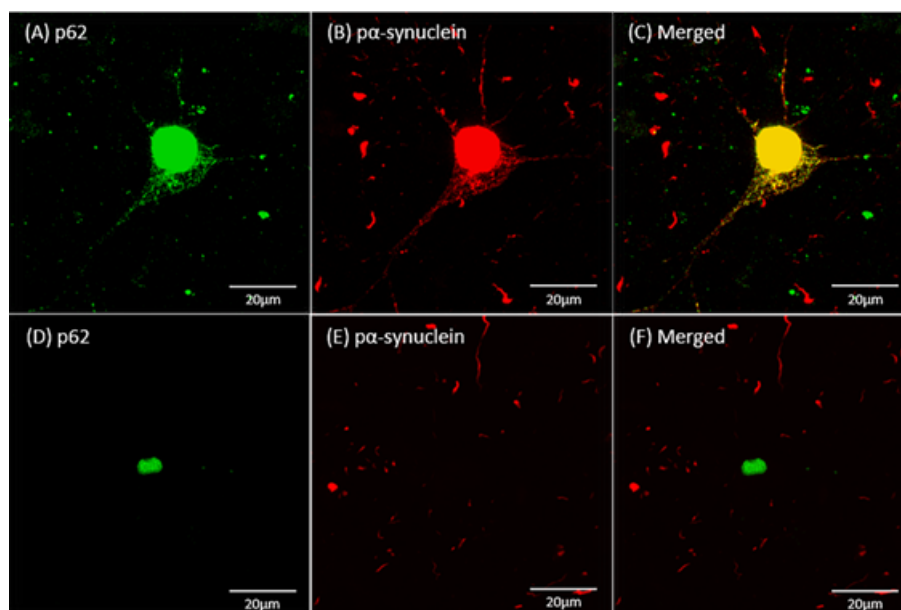

Figure 3: Immunofluorescent double labelling of p62 (green) and pα-synuclein (red) in the PD brain. Expression of p62 was observed in aggregates of different sizes known as p62 bodies (A and D). Expression of pα-synuclein was observed in a large intracellular inclusion morphologically identified as a Lewy body and some process-like structures identified as Lewy neurites (B and E). The pα-synuclein positive Lewy body was co-localised with p62, but the p62 bodies did not necessarily co-localise with pα-synuclein (C and F).

Scale bar: 20 µm

Co-pathologies of endothelium with pα-synuclein and neurons

Figure 5 shows the distributions and morphologies of endothelium co-labelled with pα-synuclein (Figures 5A-5D) and neurons (Figures 5E-5H) in both age-matched control (left panel) and PD cases (right panel). Similar to our previous report [3], the endothelial cell associated blood vessels in the PD cases were more fragmented (Figures 5B and 5G) with endothelial clusters (Figure 5, insert H) compared to the age-matched control cases (Figures 5A and 5E). The pα-synuclein positive aggregates, with various sizes and shapes were widely distributed throughout the PD cases (Figure 5B), but were much less evident in the control cases (Figure 5A). The aggregates were observed as large (general size ≥ 7µm^2) round shaped Lewy bodies (Figure 5B, insert C), dots and fibrous structures (Figure 5B, insert D). In the age-matched control cases, the NeuN positive neurons were evenly distributed with normal neuronal morphology of both cytoplasm and processes (Figure 5E, insert F). Compared to the control cases, there were fewer NeuN positive neurons that were more faintly stained with a patchy distribution indicating neuronal loss in the PD cases (Figure 5G, insert H).

To evaluate the relationship of vascular degeneration with neuronal pathology, the co-pathologies of endothelium with pα-synuclein and neurons were assessed in the same areas with DAB double labelling.
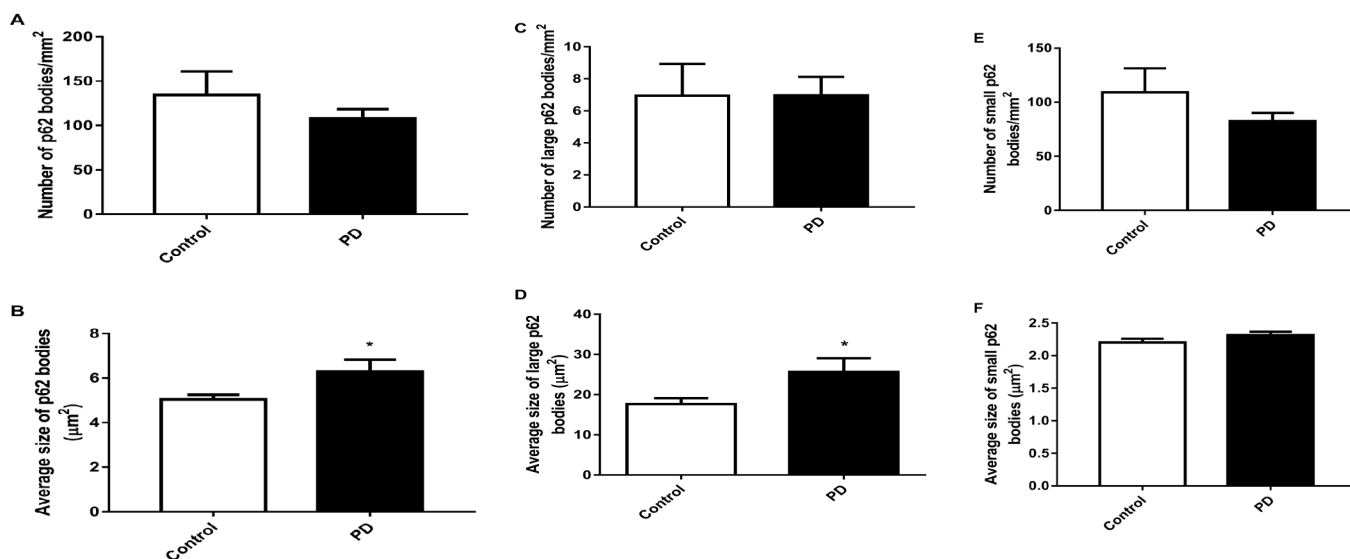
Figure 4: (A) Density and (B) average size of p62 bodies in the PD and age-matched control cases. In the PD cases, there was a significant increase in the average size of p62 bodies (B, *p<0.05) but not in density (A) of the p62 staining, compared with the age-matched control cases. There was no difference in the density (C) of p62 bodies larger than 7 μm² between the two groups but the average size (D, *p<0.05) of the large p62 bodies increased in the PD cases. There was no difference in the density (E) or average size (F) of p62 bodies smaller than 7 μm² between the two groups.

Figure 5: Double colour peroxidase-DAB immunohistochemical staining of endothelium using Factor VIII (brown) co-labelled with pα-synuclein (A-D, black) and neurons labelled with NeuN (E-H, black) respectively in both age-matched control (left panel) and PD (right panel) cases. Compared to the age-matched control case (A, E and insert F), the blood vessels in the PD case were more fragmented (B and G) with clustered endothelial morphology (insert H). Aggregates of pα-synuclein were very rare in the control case (A), but widely distributed in the PD case (B), where the aggregates were observed in forms of Lewy bodies (arrow and insert C), fine punctate staining and fibres (arrowheads and insert D). The NeuN positive neurons in the age-matched control case were evenly distributed with normal cytoplasm and process morphologies (E and insert F). In the PD case, the NeuN positive neurons were fewer; less evenly distributed and faintly stained (G and insert H). Scale bars: 100 μm and 20 μm (inserts)

The sections with more than 1000 neurons/mm^2 and less than 230 pα-syn profiles/mm^2 were specified as 'moderate' degeneration whereas locations with less than 1000 neurons/mm^2 and more than 230 pα-synuclein profiles/mm^2 were specified as 'severe' degeneration. Compared to the age-matched controls the total vessel length was reduced in the PD cases in both areas with 'moderate' (<230 pα-synuclein profiles/mm^2, $p < 0.01$, Figure 6A) and 'severe' (>230 pα-synuclein profiles/mm^2, $p < 0.001$, Figure 6A) degeneration specified by pα-synuclein number. Two-way ANOVA analysis suggested a significant difference between PD and age-matched controls ($p < 0.0001$, F $(1,21)=46.06$, Figure 6A), but there was no difference between moderate and severe degeneration, when the degree of degeneration was specified by number of existing neurons, and no interactions between the groups and severity of the degeneration. Similarly, the vessel length was reduced ($p < 0.0001$, F $(1,18)=25.4$, Figure 6B) in PD in both areas with moderate (>1000 neurons/mm^2, $p < 0.01$, Figure 6B) and severe (<1000 neurons/mm^2, $p < 0.05$, Figure 6B) degeneration. There was no difference in vessel length between the areas with moderate and severe degeneration and there was no interaction between the groups and severity of the degeneration. To investigate the relative changes of endothelial cells with pα-synuclein aggregation and neuronal loss, this study further analysed the ratios of total vessel length to pα-synuclein profile number and total vessel length to neuronal number. Two-way ANOVA suggested a significant reduction in the ratio of the

vessel length to pα-synuclein number between the groups ($p=0.003$, F $(1,21)=11.16$, Figure 6C), and significant reduction between the areas with moderate and severe degeneration ($p < 0.0001$, F $(1,21)=28.61$, Figure 6C) specified by pα-synuclein number. However, post-hoc test showed a significant decrease in the vessel length to pα-synuclein number ratio in areas with severe degeneration in both PD ($p < 0.05$, Figure 6C) and control ($p < 0.01$, Figure 6C) groups. When the degree of degeneration was specified by neuronal number the study showed a significant increase in the vessel length to neuronal number ratio in areas with severe degeneration compared to those with moderate degeneration ($p=0.005$, F $(1,18)=9.98$, Figure 6D). There was no difference in the vessel length to neuronal number ratio between the two groups. Post-hoc test suggested an increase in the vessel length to neuronal number ratio in areas with severe degeneration in the PD cases ($p < 0.05$, Figure 6D), but not in the control cases.

Iba1 positive microglia and HLADR positive activated microglia

Figure 7 shows the immunofluorescent labelling of Iba1, a marker of microglia (Figure 7A) and HLADR, a marker of microglial activation (Figure 7B). The Iba1 expression was observed in cell bodies and processes of microglia. HLADR was co-localised with Iba1 in cell bodies and processes in a subgroup of the activated microglia (Figure 7C).
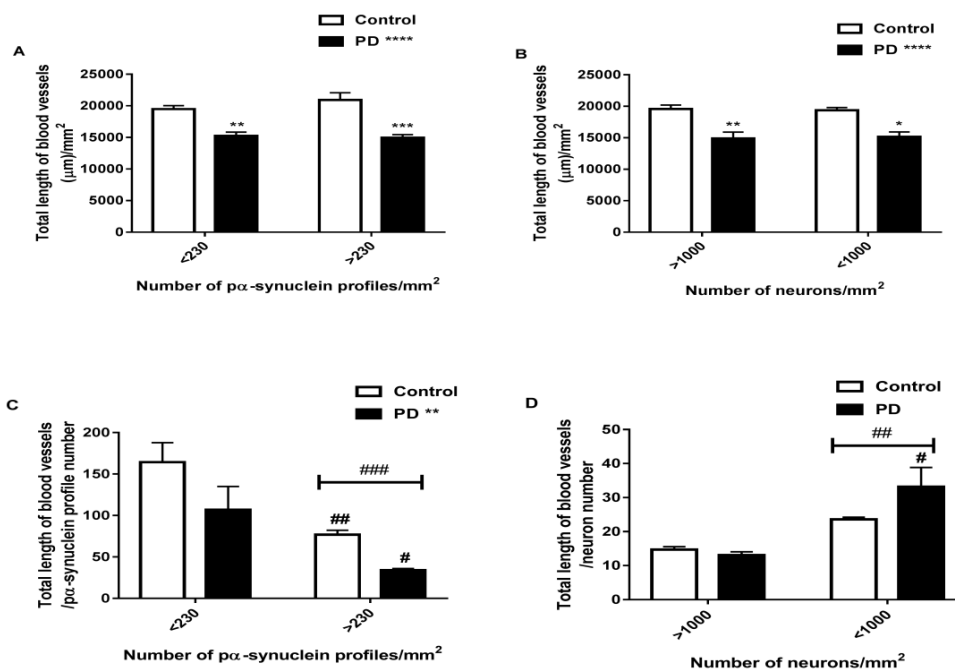

Figure 6: (A and B) Total length of endothelial cell associated blood vessels, and ratios of total length of the blood vessels to numbers of (C) pα-synuclein profiles and (D) neurons respectively in areas with different degrees of degeneration specified by pα-synuclein and neuronal densities in the PD and the age-matched control cases. There was a significant difference in total vessel length between the PD and the age-matched control groups when the degree of degeneration was specified by pα-synuclein number (A, ****$p < 0.0001$, F $(1,21)=46.06$). The total vessel length was reduced in PD in both areas with 'moderate' (<230 pα-synuclein profiles/mm^2, A, **$p < 0.01$) and 'severe' (>230 pα-synuclein profiles/mm^2, A, ***$p < 0.001$) degeneration. Similarly, there was a significant difference in total vessel length between the PD and the control groups when the degree of degeneration was specified by number of existing neurons (B, ****$p < 0.0001$, F $(1,18)=25.4$). The total vessel length was reduced in PD in both areas with moderate (>1000 neurons/mm^2, B, **$p < 0.01$) and severe (<1000 neurons/mm^2, B, *$p < 0.05$) degeneration. There was a significant reduction in the ratio of total vessel length to pα-synuclein profile number between the PD and the control groups (C, **$p=0.003$, F $(1,21)=11.16$) and between the areas with moderate and severe degeneration (C, ####$p < 0.0001$, F $(1,21)=28.61$) when the degree of degeneration was specified by pα-synuclein number. The total vessel length pα-synuclein number ratio was significantly reduced in areas with severe degeneration in both PD (C, #$p < 0.05$) and control (C, ##$p < 0.01$) groups. There was a significant increase in the ratio of total vessel length to neuronal number in areas with severe degeneration compared to those with moderate degeneration when the degree of degeneration was specified by neuronal number (D, ##$p=0.005$, F $(1,18)=9.98$). The vessel length to neuronal number ratio was increased in areas with severe degeneration only in the PD group (D, #$p < 0.05$).
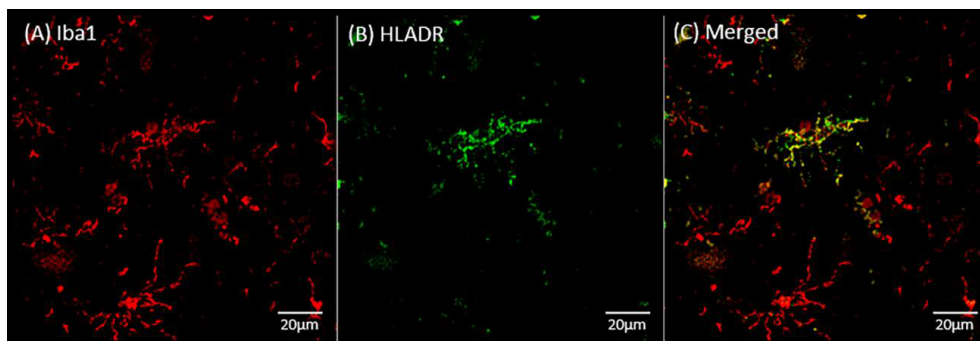
Figure 7: Immunofluorescent labelling of microglia (red) and activated microglia (green). Iba1 was expressed in cell bodies and processes of microglia (A). HLADR, a microglial activation marker (B), was co-localised with Iba1 in both cell bodies and processes of the activated microglia (C).
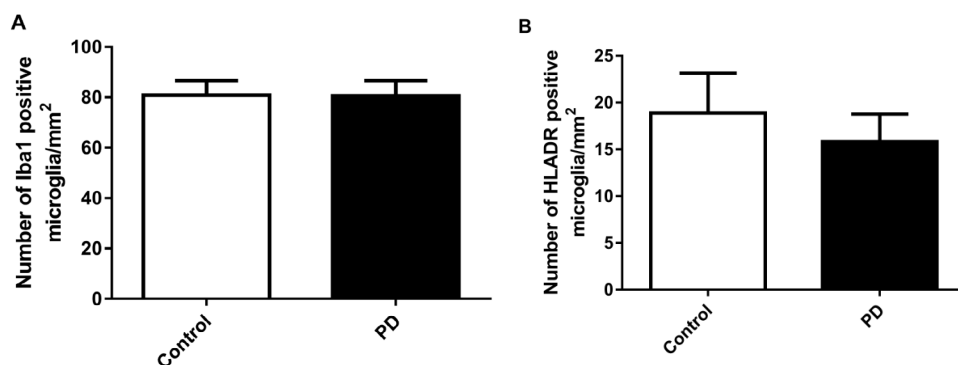

Figure 8: Densities (number/mm^2) of (A) microglia and (B) activated microglia in the PD and age-matched control cases. There was no significant difference in the densities of either Iba1 positive microglia or activated HLADR positive microglia between the two groups.

No significant difference was found in the densities (number/mm^2) of either Iba1 positive microglia or HLADR positive microglia between PD and age matched controls (Figure 8).

Discussion

The results have demonstrated that the endothelial degeneration in the MFG of the PD brains was associated with α-synuclein aggregation and autophagy impairment as measured by p62. The pα-synuclein-associated endothelial degeneration is age related and may, therefore, not be specific to PD. Endothelial degeneration is more likely to be a co-pathology of neuronal degeneration in PD. No changes were seen in microglial numbers or activation state indicating that inflammation may not be a contributing factor to neuronal and vascular degeneration in the MFG of pathologically diagnosed idiopathic PD.

The main feature of vascular degeneration in PD appears to be the degeneration of endothelial cells [3] possibly due to the impairment of vascular remodelling [5]. In this study we attempted to examine the relationships of endothelial cell degeneration with neuronal degeneration and pathology of human PD. We found increased α-synuclein and p62 aggregation with profound neuronal and endothelial cell degeneration in the grey matter of the MFG. The degree of endothelial degeneration was significantly correlated with the extent of pα-synuclein accumulation. It has been well demonstrated that α-synuclein [26] and its associated autophagy alterations [9] and inflammation [7,27,28] contribute to the pathogenesis of neuronal degeneration of PD. Regardless of the size range of the aggregates, the

pα-synuclein profiles were increased in number and size in PD brains. The findings agree with the previous reports regarding the aggregation of misfolded α-synuclein in PD [6]. Aggregation of p62 was observed in the LBs by showing co-localisation with pα-synuclein but not in the Lewy neurites. The co-expression of autophagosomes and α-synuclein has been previously reported in an *in vitro* study [8]. Some large LB-like p62 aggregates were not associated with the LBs (Figures 3F). The pathophysiological role of these large aggregates could be related to the degradation of other large intracellular materials given the broader function of p62 in autophagy [11]. The increased expression of p62 in PD group was mainly caused by large aggregates as when the analyses excluded the large LB-like p62 aggregates; neither the number nor the average size of the small p62 aggregates was different between the two groups. This implies that the accumulation of p62 or impairment of autophagy in PD could be related to the formation of LBs. A recent *in vitro* study reported that α-synuclein overexpression lead to increased level of p62 as a result of autophagy impairment [9]. Another *in vitro* study showing co-localisation of LB-like α-synuclein aggregates and p62 suggests that the LB-like α-synuclein aggregates resist degradation and impair autophagy [8]. P62 is digested together with the autophagy substrates by autophagosomes [12,13]. Our study provided the first evidence showing in human brain tissues that impaired autophagy could be associated with α-synuclein aggregation and LB formation in PD.

Using human tissues for investigating the timing of events, for example whether endothelial degeneration happens before neuronal degeneration, is limited if not impossible. Thus to investigate the

relationship of endothelial degeneration with α-synuclein pathology and neuronal loss, we assessed the co-changes of endothelial cells with pα-synuclein (Figures 5A-5D) and neurons (Figures 5E-5H), respectively. The co-pathology between the PD and age-matched control groups were compared using DAB double labelled sections. The age matched control cases used also had mild neuronal and endothelial degeneration, as well as age-related pathologies, for example α-synuclein and p62 expression. The PD cases however showed more severe endothelial degeneration, neuronal degeneration and increased pα-synuclein. The increase of pα-synuclein was strongly correlated to the endothelial degeneration in both PD and age-matched controls (Figure 1D). The α-synuclein pathology and its association with neuronal degeneration are characteristic of PD. This study provided evidence of the association of α-synuclein with endothelial cell degeneration in PD.

Endothelial degeneration leads to an increase in the formation of string vessels which are unable to function in blood circulation [4], thus a possible role for vascular dysfunction in contributing to secondary neuronal loss in PD was proposed. It is a difficult task to evaluate the timing of events during the disease process and whether vascular degeneration would be a contributor or the outcome of neuronal degeneration or simply the co-pathology in PD. To answer these questions the study would require human brain tissues at different stages of the disease development. But with post-mortem human tissue, it is often difficult to have enough subjects available at each stage of the disease, especially when there is not a clear criterion for the early stages of PD. However, the degree of neuronal degeneration and a-synuclein aggregation in PD is not uniform in an individual brain or a large brain region. Thus we hypothesised that the endothelial degeneration may be differentially related to neuronal degeneration and α-synuclein aggregation in the areas with severe or moderate degenerative pathology. The grey matter of MFG is a large region where the degree of degeneration varied considerably. We classified the severity of the pathology according to the densities of α-synuclein aggregates (<230 or >230 pα-synuclein profiles/mm^2) and neurons (>1000 or <1000 neurons/mm^2) in specified areas with double labelling of either endothelium/neuron or endothelium/pα-synuclein in both PD and age-matched controls. The loss of endothelial cells that was measured as total length of vessels, in PD cases did not correspond to the severity of either α-synuclein aggregation (Figure 6A) or neuronal loss (Figure 6B). We also analysed the ratios of endothelium to either pα-synuclein or neuronal density in the same images from double labelled sections. The analysis revealed more significant loss of vessel length in the areas with severe pα-synuclein aggregation than the areas with moderate aggregation, surprisingly of both PD and age-matched control groups. The data suggested the relative changes of endothelium to pα-synuclein aggregation were not a PD specific, rather an age-related pathology given PD is an age related condition.

Although the α-synuclein pathology is a defining marker in PD, it also appeared in some of the age-matched control cases, even though the level of the α-synuclein deposition was lower (Figure 2) [29]. Without a young control group to compare, the evaluation of the relative changes of α-synuclein to endothelial cells may help to reveal the change with age.

The relative changes of vascular length to neuronal number were increased in the tissue with more severe neuronal degeneration particularly in the PD cases (Figure 6D). The results may suggest that the blood vessel degeneration is slower than the neuronal loss in the brain or is a compensatory response through improved vascular remodelling. Therefore, the evidence suggests that during the

pathological progression of PD, the neuronal loss is likely to precede the vascular degeneration.

The relationships among α-synuclein aggregation, neuronal loss and blood vessel changes may be dynamic. Observing the ratios in the areas with different degrees of pathology may provide an initial insight into the relationship between these pathological features through disease progression. Our current observation may suggest that the increased α-synuclein aggregation may not be a cause or the result, rather the co-pathology of vascular degeneration due to advanced age. However, the significant change in relationship of endothelial cells to neuronal degeneration was observed only in PD brains.

Accumulating evidence suggests the role for inflammation in neuronal degeneration of PD, particularly in the SN of the PD brain, where activation of microglia has been suggested to contribute to the death of dopaminergic neurons [7]. However we did not see higher levels of microglial activation in the MFG of the PD cases (Figure 8). This may suggest that there was no inflammation in the MFG of the PD cases. We have previously reported that the BBB function is maintained in the MFG of these PD cases due to the retained basement membrane [4]. It is likely that the retained BBB [4] has played a key role in preventing the inflammation in PD brains [30].

The current study analysed the MFG region where the BBB is not leaking and shows no astrocytosis [4]. Thus the relationship of neuronal, vascular and pathological changes, for example α-synuclein aggregation and inflammation may be different in the brain regions with BBB leakage and activation of glia, such as the CN [4], which needs to be evaluated in a separated study.

Conclusion

In conclusion, α-synuclein aggregation and autophagy impairment, but not inflammation, were related to endothelial degeneration in PD. The α-synuclein-associated endothelial degeneration is not specific to PD itself, but is rather an age-related pathology, which nevertheless is more severe in PD compared with the aged controls.

References

1. de Lau LM, Breteler MM (2006) Epidemiology of Parkinson's disease. Lancet Neurol 5: 525-535.

2. Savitt JM, Dawson VL, Dawson TM (2006) Diagnosis and treatment of Parkinson's disease: Molecules to medicine. J Clin Invest 116: 1744-1754.

3. Guan J, Pavlovic D, Dalkie N, Waldvogel HJ, O'Carroll SJ, et al. (2013) Vascular degeneration in Parkinson's disease. Brain Pathol 23: 154-164.

4. Yang P, Pavlovic D, Waldvogel H, Dragunow M, Synek B, et al. (2015) String vessel formation is increased in the brain of Parkinson's disease. J Parkinson'ss Dis 5: 821-836.

5. Yang P, Waldvogel H, Turner C, Faull R, Dragunow M, et al. (2017) Vascular remodelling is impaired in Parkinson's disease. J Alzheimers Dis Parkinsonism 7.

6. Venda LL, Cragg SJ, Buchman VL, Wade-Martins R (2010) α-Synuclein and dopamine at the crossroads of Parkinson's disease. Trends Neurosci 33: 559-568.

7. Hirsch EC, Hunot S (2009) Neuroinflammation in Parkinson's disease: A target for neuroprotection? Lancet Neurol 8: 382-397.

8. Tanik SA, Schultheiss CE, Volpicelli-Daley LA, Brunden KR, Lee VMY (2013) Lewy body-like α-synuclein aggregates resist degradation and impair macroautophagy. J Biol Chem 288: 15194-15210.

9. Winslow AR, Chen CW, Corrochano S, Acevedo-Arozena A, Gordon DE, et al. (2010) α-Synuclein impairs macroautophagy: Implications for Parkinson's disease. J Cell Biol 190: 1023-1037.

10. Anderson JP, Walker DE, Goldstein JM, De Laat R, Banducci K, et al. (2006) Phosphorylation of Ser-129 is the dominant pathological modification of α-synuclein in familial and sporadic lewy body disease. J Biol Chem 281: 29739-29752.

11. Pankiv S, Clausen TH, Lamark T, Brech A, Bruun JA, et al. (2007) p62/SQSTM1 binds directly to Atg8/LC3 to facilitate degradation of ubiquitinated protein aggregates by autophagy*[S]. J Biol Chem 282: 24131-24145.

12. Bjørkøy G, Lamark T, Brech A, Outzen H, Perander M, et al. (2005) p62/SQSTM1 forms protein aggregates degraded by autophagy and has a protective effect on Huntington-induced cell death. J Cell Biol 171: 603-614.

13. Komatsu M, Waguri S, Koike M, Sou YS, Ueno T, et al. (2007) Homeostatic levels of p62 control cytoplasmic inclusion body formation in autophagy-deficient mice. Cell 131: 1149-1163.

14. Cameron B, Landreth GE (2010) Inflammation, microglia and Alzheimer's disease. Neurobiol Dis 37: 503-509.

15. Ransohoff RM, Cardona AE (2010) The myeloid cells of the central nervous system parenchyma. Nature 468: 253-262.

16. Block ML, Hong JS (2005) Microglia and inflammation-mediated neurodegeneration: Multiple triggers with a common mechanism. Prog Neurobiol 76: 77-98.

17. Di Marco LY, Venneri A, Farkas E, Evans PC, Marzo A, et al. (2015) Vascular dysfunction in the pathogenesis of Alzheimer's disease-A review of endothelium-mediated mechanisms and ensuing vicious circles. Neurobiol Dis 82: 593-606.

18. Brown WR, Thore CR (2011) Review: Cerebral microvascular pathology in ageing and neurodegeneration. Neuropathol Appl Neurobiol 37: 56-74.

19. Waldvogel HJ, Curtis MA, Baer K, Rees MI and Faull RLM (2007) Immunohistochemical staining of post-mortem adult human brain sections. Nat Protoc 1: 2719-2732.

20. Bourdenx M, Dovero S, Engeln M, Bido S, Bastide MF, et al. (2015) Lack of additive role of ageing in nigrostriatal neurodegeneration triggered by α-synuclein overexpression. Acta Neuropathol Commun 3: 46.

21. Scotter EL, Vance C, Nishimura AL, Lee YB, Chen HJ, et al. (2014) Differential roles of the ubiquitin proteasome system and autophagy in the clearance of soluble and aggregated TDP-43 species. J Cell Sci 127:1263-1278.

22. Rangaraju S, Gearing M, Jin LW, Levey A (2015) Potassium channel Kv1.3 is highly expressed by microglia in human Alzheimer's disease. J Alzheimers Dis 44: 797-808.

23. Prinz M and Priller J (2017) The role of peripheral immune cells in the CNS in steady state and disease. Nat Neurosci 20: 136-44.

24. Dragunow M (2008) High-content analysis in neuroscience. Nat Rev Neurosci 9: 779-788.

25. Narayan PJ, Kim SL, Lill C, Feng S, Faull RLM, Curtis MA, et al. (2015) Assessing fibrinogen extravasation into Alzheimer's disease brain using high-content screening of brain tissue microarrays. J Neurosci Methods 247: 41-49.

26. Yasuda T, Nakata Y, Mochizuki H (2013) α-Synuclein and neuronal cell death. Mol Neurobiol 47: 466-483.

27. Liu B, Jiang JW, Wilson BC, Du L, Yang SN, et al. (2000) Systemic infusion of naloxone reduces degeneration of rat substantia nigral dopaminergic neurons induced by intranigral injection of lipopolysaccharide. J Pharmacol Exp Ther 295: 125-132.

28. Vila M, Jackson-Lewis V, Guégan C, Chu Wu D, Teismann P, et al. (2001) The role of glial cells in Parkinson's disease. Curr Opin Neurol 14: 483-489.

29. Jellinger KA (2004) Lewy body-related α-synucleinopathy in the aged human brain. J Neural Transm 111: 1219-1235.

30. Kim SY, Buckwalter M, Soreq H, Vezzani A, Kaufer D (2012) Blood-brain barrier dysfunction-induced inflammatory signaling in brain pathology and epileptogenesis. Epilepsia 6: 37-44.